Food & Function

Accepted Manuscript

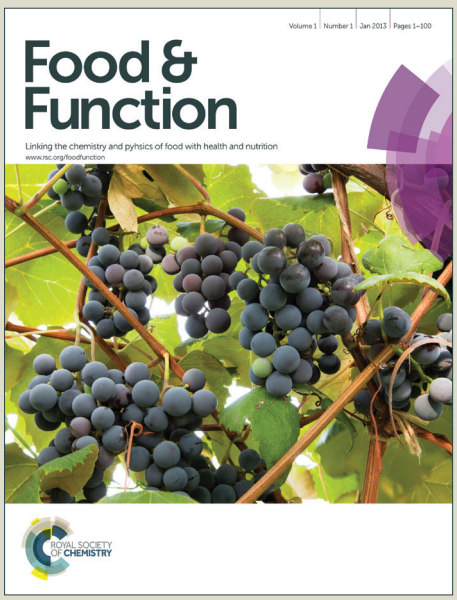

This is an *Accepted Manuscript*, which has been through the Royal Society of Chemistry peer review process and has been accepted for publication.

Accepted Manuscripts are published online shortly after acceptance, before technical editing, formatting and proof reading. Using this free service, authors can make their results available to the community, in citable form, before we publish the edited article. We will replace this *Accepted Manuscript* with the edited and formatted *Advance Article* as soon as it is available.

You can find more information about *Accepted Manuscripts* in the Information for Authors.

Please note that technical editing may introduce minor changes to the text and/or graphics, which may alter content. The journal's standard Terms & Conditions and the Ethical guidelines still apply. In no event shall the Royal Society of Chemistry be held responsible for any errors or omissions in this *Accepted Manuscript* or any consequences arising from the use of any information it contains.

ROYAL SOCIETY OF CHEMISTRY

www.rsc.org/foodfunction

On characterization of anisotropic plant protein structures

Georgios A. Krintiras[1], Jesse Göbel[1], Wim G. Bouwman[2], Atze Jan van der Goot[3], Georgios D. Stefanidis[1,*]

[1] Delft University of Technology, Process & Energy Department, Leeghwaterstraat 39, 2628 CB Delft, The Netherlands

[2] Delft University of Technology, Neutron and Positron Methods in Materials, Mekelweg 15, 2629 JB Delft, the Netherlands

[3] Food Process Engineering Group, Wageningen University and Research, P.O. Box 176700 AA, Wageningen, The Netherlands

*Corresponding author. Tel.: +31 15 27 81 447, E-mail address: G.Stefanidis@tudelft.nl (Georgios D. Stefanidis).

Abstract

In this paper, a set of complementary techniques was used to characterize surface and bulk structures of an anisotropic Soy Protein Isolate (SPI) – vital wheat gluten blend after it was subjected to heat and simple shear flow in a Couette Cell. The structured biopolymer blend can form a basis for a meat replacer. Light microscopy and scanning electron microscopy provided a detailed view of structure formation over the visible surfaces of the SPI-gluten blend. Protein orientation in the direction of the flow was evident and fibrous formation appeared to exist in the macro- and micro-scale. Further, according to texture analysis, the structured biopolymer obtained from the Couette Cell after processing at 95^{o}C and 30 RPM for 15 min has high tensile stress and strain anisotropy indices (~2 and ~1.8, respectively), comparable to those of raw meat (beef). The novel element in this work is the use of the neutron refraction method, utilizing spin-echo small angle neutron scattering (SESANS), to provide a *look inside* the anisotropic biopolymer blend complementing the characterization provided by the standard techniques above. With SESANS, it is possible to quantify the number of fibre layers and the orientation distribution of fibres. For a specimen thickness of 5 mm, the obtained number of fibre layers was 36 ± 4 and the standard deviation of the orientation distribution was 0.66 ± 0.04 radians. The calculated thickness of one layer of fibres was 138 μm in line with SEM inspection.

Keywords: food characterization, meat replacer, Couette Cell, soy, gluten, plant protein, neutron refraction

1. *Introduction*

Meat production has an enormous impact on the environment and natural resources. According to a 2006 study by the United Nations Food and Agriculture Organization (FOA) [1], 18% of the annual worldwide Greenhouse Gas (GHG) emissions are attributed to livestock (cattle, buffalo, sheep, goats, camels, horses, pigs, and poultry). This is higher than the contribution of transportation emissions (13%) on global scale [2]. Similar claims can be made for land use and water footprint. Besides, the issue of animal welfare is another major concern. Clearly, there is need to reduce meat consumption. From consumer research, it becomes clear that they are prepared to switch to plant-based alternatives, provided that these resemble meat more accurately. Unfortunately, current meat replacers do not meet all consumer wishes or are too expensive [3]. Further development of meat replacers is also hindered by lack of analytical methods that allow inspection of structures inside the products.

Currently, extrusion and spinning, are the main techniques available to produce anisotropic structured meat replacers[4, 5]. Recently, two new techniques based on the concept of flow-induced structuring were introduced. A cone-cone device (Shear Cell) [6] and a concentric cylinder device (Couette Cell) [7] were developed. A model system of Soy Protein Isolate (SPI) and vital wheat gluten blend has been used in both devices yielding anisotropic structures that can serve as meat replacers.

Several characterization techniques, such as light microscopy (LM), scanning electron microscopy (SEM) and texture analysis (TA) [8, 9] are typically used to extract information regarding food structures we produce or consume. LM and SEM characterize food sample surfaces. TA can be used to quantify mechanical properties (stresses and strains) and the anisotropy of food samples. In this work, we introduce the neutron refraction method with the technique of Spin-Echo Small Angle Neutron Scattering (SESANS) [10, 11] as a new characterization method of anisotropic biopolymer blends, such as soy protein isolate and vital wheat gluten. SESANS can be used to quantify the number and thickness of fibrous layers inside the material and should be seen as a complementary method to LM, SEM and TA.

In order for analysis of the bulk structure of a material, a *look inside* is required. To this end, regular light is sufficient in case of transparent materials, but for opaque materials, different techniques need to be used. Refraction is defined as the change in direction of a wave (or neutron) due to a change in the optical medium. When a neutron

passes through a sample, containing structures of material that is different than the surrounding material, refraction can occur. When structures inside a sample are relatively large (much larger than the coherence length of the neutron in the instrument [10]), the effect of refraction is predominant over scattering.

A technique that can measure neutron refraction is called SESANS standing for Spin Echo Small Angle Neutron Scattering. Neutrons are refracted by the scattering length density variations, due to different concentrations of isotopes. Neutron refraction is useful for the study of biopolymer structures in that the isotopic scattering length *b* has a large negative value, -3.742 fm, for hydrogen (^{1}H), compared with 6.671 fm for deuterium (^{2}H), 6.651 fm for carbon (^{12}C), 9.400 fm for nitrogen (^{14}N) and 5.804 fm for oxygen (^{16}O) [12]. Therefore, important (biological) elements with low atomic numbers like hydrogen, carbon and oxygen are well visible in neutron refraction. This renders neutron refraction a suitable method for study of proteins since these molecules are mostly made up of hydrogen, carbon, nitrogen and oxygen.

Refraction depends on the number of interfaces (density changes) the beam has to pass through and the shape of the interfaces. For example, when a fibre is placed perpendicular to the direction of a neutron beam, a neutron changes direction when passing the air - metal interface and again when leaving the wire through the metal - air interface. Consequently, the distance travelled within the wire does not influence refraction and the diameter of the wire does not influence the final deviation of the neutron from the incoming direction. Assuming that the fibres (in meat or soy) can be modelled as cylindrically shaped wires and that these fibres are composed of material (proteins) other than the material that surrounds them (e.g. air or heavy water), the principle of refraction can be used to obtain information on fibrous materials. Plomp et al.[10] described the theory of neutron refraction by cylindrical metal wires, which can be used as a basis for the interpretation of SESANS measurements on fibrous materials.

2. Materials and recipe

A blend of soy protein isolate (SPI) (SUPROR EX37 HG IP, Solae, USA) and vital wheat gluten (WG) (VITENR, Roquette, France) was used. According to the manufacturer specification, SPI has a minimum protein content of 90% on a moisture-free basis, while gluten contains a minimum of 83% proteins on dry basis. Analysis for comparison was performed on beef (specifically the blade, which is part of the chuck; front part of the cow). Each SPI/gluten and

raw meat sample was packaged in a seal bag and was stored in a freezer (at -20 ^{o}C). Samples were defrosted prior to further analysis.

All characterization methods were applied to samples prepared with the same recipe (Table 1) and procedure. The mixture created had a dry matter content of 31 wt%, with an SPI-gluten ratio of 3.3:1. First, the demi-water-salt solution was made and added to SPI. The mixture was manually mixed with a spatula and then rested for 30 minutes. Finally, gluten was added followed by mixing with the spatula.

Table 1: Ingredients for recipe preparation.

Ingredients	w/w [%]
Soy Protein Isolate	23
Demi - water	69
Salt (sodium chloride)	1
Gluten	7
Total	100

3. Preparation of structured samples in a Couette Cell

The protein mixture consists of deformable granules. A transparent (caulking) filling gun container using a funnel and a pounder is employed to fill the Couette Cell with the material. The Couette Cell is filled from the side using a filling tube that is screwed onto the filling hole. When the space between the cylinders (shearing zone) was completely filled, the filling tube was removed and the filling hole was sealed using a screw plug with a thermocouple attached. Then, the experiment was started as fast as possible.

The Couette Cell [7, 13] is a concentric cylinder device comprising an inner rotating cylinder (R_i = 0.0425 m) and an outer cylinder (R_o = 0.0485 m), which remains stationary. Both the inner and outer cylinders are heated by means of oil. The sample material is placed in the space between the two cylinders (gap size = 0.006m); this space is called shearing zone. The height of both cylinders is H = 0.085 m.

During a previous study [7], several samples with the composition of Table 1 were processed in the Couette Cell at different process conditions (temperature, rotation speed (RPM) and process time). The products were characterized afterwards by means of TA and SEM. It was found that samples processed for 15 min at 95 ^{o}C and 30 RPM yielded

products with high Anisotropic Indices (AI). These samples had distinct anisotropic structures present and, in particular, fibrous structures. A detailed overview of the device used and the experiments performed can be found in the experimental parametric study by [7].

4. *Characterization methods*

4.1. *Light Microscopy*

The microscope used is a Nikon Optiphot 200 (Nikon Corporation, Tokyo, Japan), which comes with CF Plan BD 5/10/20/50x objectives for bright and dark fields and the possibility to obtain images with a digital camera, mounted on the eyepiece tube, and a rotating diascopic polarizer. The light microscope has been used to observe structured samples. The observations took place at room temperature and provisions were taken to ensure that limited drying of the samples occurred. Specifically, samples have been kept in airtight compartments with glass windows. Samples were strained using toluidine blue stain moutant, which enabled visual differentiation between the two plant proteins (SPI, gluten) used in the study [14]. A couple of droplets of toluidine were applied to the surface and the specimen, which was then left to rest for a couple of minutes. Toluidine stained the SPI protein with a dark purple-blue colour and the wheat gluten with a pale blue-green colour.

4.2. *Scanning Electron Microscopy*

The micro- and nanostructures of the samples were investigated with SEM (JSM-5400, Jeol, Tokyo, Japan). The specimens were coated with an ultra-thin layer of gold with an ion sputter coater (JFC-1100E, Jeol, Tokyo, Japan) in order for the surface of the specimens to become electrically conductive. The SEM at hand features high resolution and low voltage imaging with a maximum resolution of 4.0 nm and a variable acceleration voltage of 0.5 - 30 kV. Both secondary electron and backscattering electron detectors are available for imaging.

4.3. *Texture Analysis-Mechanical Testing*

Tensile tests were performed on a Zwick Roell Z005 universal testing machine (Zwick Roell AG., Ulm, Germany) to determine the degree of stress and strain anisotropy in the obtained samples. As shown in Figure 1, "parallel" is defined by the vector v (direction of velocity in the Couette Cell) and "perpendicular" by vector H (height of Couette Cell). Defrosted SPI/gluten samples and raw meat (beef) were subjected to texture analysis.

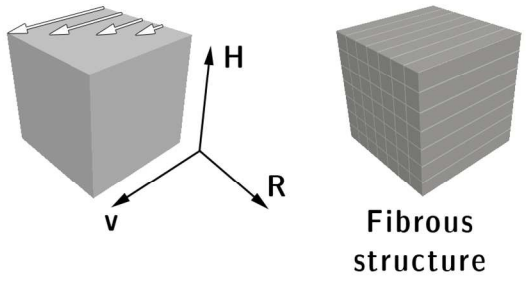

Figure 1: Schematic display of the orientation of fibrous structures related to the direction of flow in the Couette Cell. H is the height, R is the radius and v is the direction of velocity in the device.

The tensile tests were performed with a constant deformation rate of 0.5 mm s^{-1} at room temperature. Three samples have been used and at least three test specimens per direction were cut from each sample at the locations indicated in Figure 2. The specimens were cut in rectangular shape (85 x 5.5 mm) with a thickness of 5.5 mm. Thus, the cross sectional area relevant for calculating the normal stress was $3.025 \cdot 10^{-5}$ m^2.

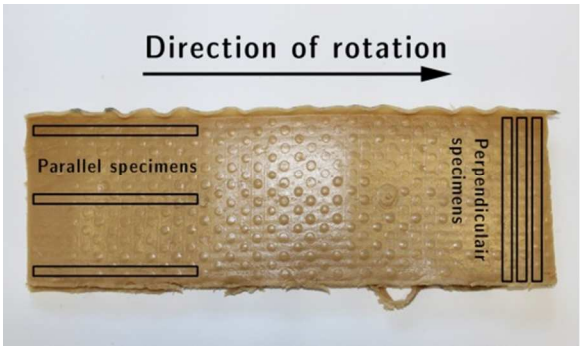

Figure 2: Locations on sample where cuts were made for texture analysis. The surface pattern is a result of the dimples on the surface of both the inner and outer cylinder made to avoid slip.

Roller clamps with a rough surface were used to fixate the specimens in the tester. The roller clamps press the specimens against a piece of sanding paper glued onto a metal plate. The rollers were fitted with rubber rings of 3

mm thickness to prevent excessive compression of the specimens. The distance between the points of application of the rollers was 58.34 mm. This distance was used to calculate the tensile strain. The force, distance, tensile stress and strain were recorded using Zwicks testXpert® software.

The maximum values for tensile stress and strain were determined for each specimen. The maximum tensile strain is determined at the point of maximum tensile stress. The maximum tensile stress and strain per direction were averaged and the relevant anisotropy indices (AI) were calculated through Equations 1 and 2, respectively.

$$AI_{\sigma} = \frac{\sigma_{\square}}{\sigma_{\perp}} \qquad (1)$$

where AI_{σ}[-] is the stress anisotropy index; $\sigma_{||}$[Pa] is the normal stress for specimens cut parallel to the fibres and $\sigma_{\perp}$[Pa] is the normal stress for specimens cut perpendicular to the fibres

$$AI_{\varepsilon} = \frac{\varepsilon_{\square}}{\varepsilon_{\perp}} \qquad (2)$$

where, AI_{ε}[-] is the strain anisotropy index; $\varepsilon_{||}$ [mm/mm] is the normal strain for specimens cut parallel to the fibres and $\varepsilon_{\perp}$ [mm/mm] is the normal strain for specimens cut perpendicular to the fibres.

4.4. Neutron refraction detected by spin-echo

4.4.1. Sample preparation

One sample was tested in the SESANS instrument located at the Reactor Institute Delft (RID). The sample selected was the one with the most pronounced fibrous structure based on visual inspection. This sample had an anisotropy index of AI_{σ}=3.16.

The partly frozen sample was cut parallel to the flow plane, which is the plane defined by vector v and H in Figure 1, into slices with a thickness of 3.5 mm for the horizontally oriented specimen and 1.5 mm for the vertically oriented specimen. After cutting, the sample was rested to allow complete defrosting. The thickness difference is corrected

during the fitting procedure of the experimental data. Two specimens were cut per slice with a circular die cutter. The specimens were placed into round transparent airtight containers, which were mounted on a specimen holder.

One specimen was placed in the specimen holder with the fibres orientated perpendicular to the sensitive direction of the instrument, i.e. with the fibres in the y-direction as shown in Figure 3, and the other one was placed in the specimen holder with the fibres orientated parallel to the sensitive direction of the instrument. Both specimens were measured for 6 h.

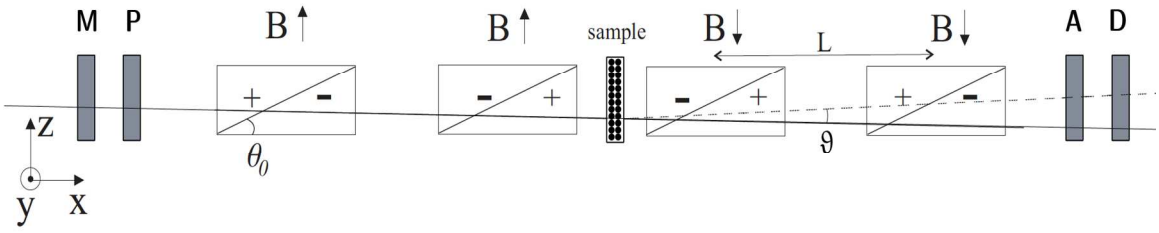

Figure 3: Schematic monochromatic SESANS arrangement with monochromator (M) polariser (P), flipper magnets (B), analyser (A) and detector (D), adapted from [10].

4.4.2. Fitting Method

The result of a SESANS measurement is a set of data points that relate the polarization, $P(B,\lambda)$ to the magnetic induction, B in each of the flipper magnets and the wavelength λ. For the analysis in this study, λ is constant. The polarization for n layers of fibres is given by:

$$P(B,\lambda) = \left(\kappa K_1(\kappa)\right)^n \qquad (3)$$

where $K_1(\kappa)$ is the first-order modified Bessel function of the second kind and κ is a scanning parameter expressed in Equation 4.

$$\kappa = 2\delta c L \cot\theta_0 B\lambda \qquad (4)$$

where $c\,[T^{-1}m^{-2}]$ is the Larmor precession constant, $c = 4.632 \cdot 10^{14}\ T^{-1}m^{-2}$, $L[m]$ is the length between the centres of the two magnetized foil flippers in each magnetic arm and $\theta_0\,[rad]$ is the inclination angle in the SESANS device.

As described before, the way neutrons are refracted depends on the shape and the number of structures that cause the refraction. When introducing the refractive index η for thermal neutrons, Equation 5 is obtained.

$$\eta = 1 - \delta \qquad (5)$$

where the deviation δ from 1 is given by:

$$\delta = \frac{\rho \lambda^2 \bar{b}}{2\pi} \qquad (6)$$

where $\rho\,[m^{-3}]$ is the number of nuclei per unit volume; $\lambda\,[m]$ is the wavelength of a neutron; $\bar{b}\,[m]$ is the mean coherent scattering length, which is positive for most materials and the product $\rho\bar{b}\,[m^{-2}]$ is the scattering length density (SLD). Since $\bar{b}$ is positive, n is less than 1; this means that a cylinder will act as a lens with a negative focal length in the direction perpendicular to the cylinder axis.

From Equations 3, 4 and 6, it can be deduced that polarization is not dependent on the diameter of the fibres, but, rather, on the material of the sample (SLD) and the number n of layers of fibres in the sample. The SLD and n have a similar effect on the calculated polarization.

Measurements in this study were done on a monochromatic SESANS instrument with a wavelength of $\lambda = 0.2 \cdot 10^{-9}$ m (2.0 Å). Since the number of layers in a sample and the composition of the fibres are unknown, Equation 3 must be fitted to the measurement data. The fitting parameters are the number of layers, n and the normalized Gaussian distribution of angles $\varphi(\alpha)$ with a standard deviation σ.

To get an idea of how a polarization curve looks like, Equation 3 is evaluated for different layers of wires, n, with a composition based on calculated SLD, displayed in Figure 4. This Figure illustrates that a specimen without fibres,

or with fibres, oriented parallel to the sensitive direction of the instrument - i.e. with the fibres in the z-direction as shown in Figure 3 - will not show depolarization. Multiple layers of fibres will increase the depolarization.

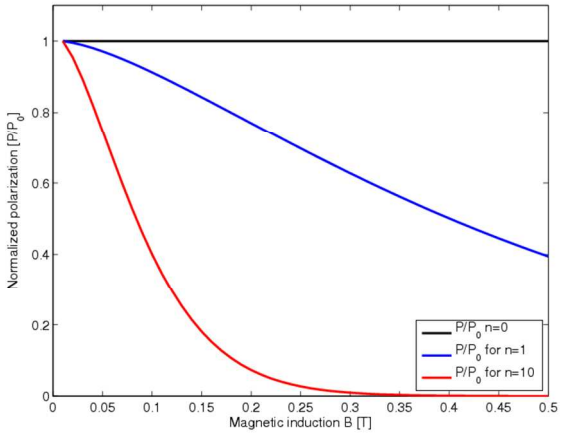

Figure 4: Equation 3 evaluated for different layers of wires, n .

The exact composition of the fibres is unknown; it can be pure SPI, pure gluten or an SPI - gluten mixture with H_2O and salt in any ratio. An initial guess for the SLD can be made assuming that the fibres consist of SPI only.

The SLD of SPI can be calculated with the SLD calculator on the website of the National Institute of Standards and Technology (NIST) [15]. The calculator on this website uses Equation 7 for calculating the SLD.

$$SLD = \frac{\sum_{i=1}^{n} b_c}{v_m} \qquad (7)$$

where $b_c\,[m]$ is the bound coherent scattering length of the i^{th} of n atoms in a molecule with molecular volume $v_m\,[m^3/mol]$. In the calculator, the empirical formula of the material is needed to determine the right values for b_c and v_m.

We have determined the bulk empirical formula of SPI to be $C^{196}H^{380}N^{51}O^{102}S^{1}$. For the calculation of the SLD, the density of the fibrous material is needed as well. Not all the densities of the amino acids are known; however, looking at the densities that are known, it is assumed that the average density is in the order of 1.5 g/cm^3 [16].

Using the above empirical formula and density in the SLD calculator, we can get a calculated value for the SLD_{SPI} of $1.68 \cdot 10^{-6}$ Å^{-2} ($1.68 \cdot 10^{14}$ m^{-2}). In addition, SLD_{air}=0 and the $SLD_{D2O} = 6.38 \cdot 10^{14}$ m^{-2}. From the SLD_{SPI}, SLD_{air} and SLD_{D2O}, we can define the lower and upper limits of SLD for our system with the lower one being the SPI/air interface of $1.68 \cdot 10^{14}$ m^{-2} and the upper one being the SPI/D_2O interface of $4.7 \cdot 10^{14}$ m^{-2}.

The SLD of both the vertical and horizontal specimens is equal since they are cut out of the same sample. The vertical specimen has a thickness of 1.5 mm compared to 3.5 mm for the horizontal specimen. Since the number of layers is proportional to the thickness, the number of layers in the sample can be calculated.

With the calculated value of the SLD and the density, Equation 3 can be fitted to the measurement data. The fitting method used is the common minimization function in MATLAB called fminsearch, which finds the local minimum of a function of several variables, starting at an initial estimate.

4.4.3. Effect of orientation of the fibres

The orientation of the specimen in the specimen holder is important because the SESANS device is only sensitive to refraction in the xz - plane. This means that when the vertical specimen (with fibres oriented in the z direction) is rotated with a small angle $\alpha < 1^{\circ}$ in the yz - plane, it will cause a small amount of refraction in the xz - plane. The depolarization caused by this refraction is calculated by scaling κ in Equation 4 with $cos\,\alpha$. The alignment of the horizontal specimen is less important given the fact that κ scales with a cosine. At $\chi = 90$ (vertical position), $\cos(\alpha - \chi)$ has a maximum slope compared to $\chi = 0$ (horizontal position) where the slope of $\cos(\alpha)$ is at a minimum. To verify how sensitive the method is to misalignment, Figure 5 shows how the polarization curve shifts from its original position, the line y=1, if a vertical specimen with 10 layers of fibres is rotated at various angles in the yz-plane.

At 1°, no significant depolarization is calculated, but at 5°, high depolarization should be visible. This shows that the results obtained by SESANS for the vertical specimens are very sensitive to alignment, implying that it is a useful

method to measure the orientation distribution. In our case, both vertically and horizontally placed specimens showed different depolarization, which indicates a finite orientation distribution.

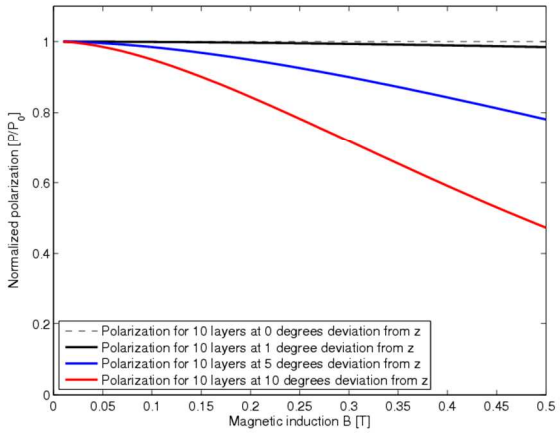

Figure 5: Theoretical polarization curves for specimens at various deviation angles assuming a specimen with 10 layers of wires and the calculated SLD.

Now the deviation angle, α, is used as a fitting parameter in Equation 3, where κ is defined as

$$\kappa = \cos(\alpha - \chi) 2\delta \mathrm{c} L \cot\theta_0 B\lambda \qquad (8)$$

This fit finds its optimum if we assume that the fibres in the specimen are not perfectly parallel to each other. In fact, there is actually a normalized Gaussian distribution of angles $\varphi(\alpha)$ with a standard deviation σ.

$$\varphi(\alpha) = \frac{e^{-\left(\frac{\alpha^2}{2\sigma^2}\right)} + e^{-\left(\frac{(a-\pi)^2}{2\sigma^2}\right)}}{2\sigma\sqrt{2\pi}} \qquad (9)$$

In Equation 9, we take into account the contribution of the same anti-parallel orientation to the distribution in order to avoid discontinuities at $\alpha = \pi/2$.

5. Results

5.1. *Light Microscopy*

Figure 6 shows LM images of a structured sample at 5x and 10x magnification. We observe that the stained proteins follow a certain direction indicating anisotropic structure formation. A closer look at the picture reveals that lighter parts in the sample are enrobed with a stranded continuous network. Possibly, this corresponds with SPI being dispersed in a continuous gluten matrix [6]. The LM indicated evidence for existence of anisotropic structures.

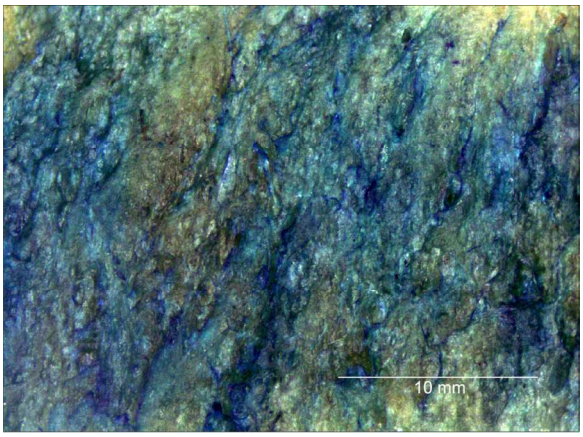

Image of a structured sample at 5x magnification

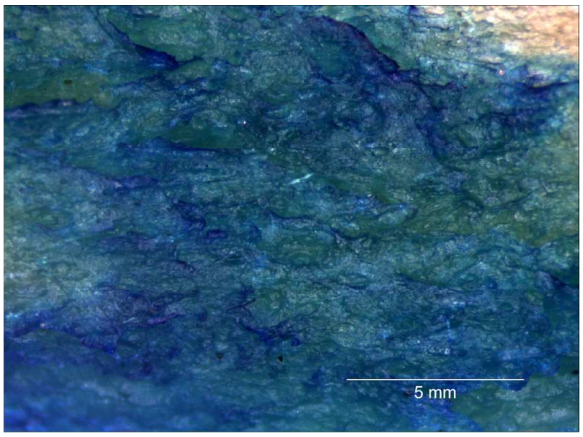

Image of a structured sample at 10x magnification

Figure 6: Images of structured sample using toluidine blue stain moutant (dark purple-blue colour for the SPI protein and pale blue-green colour for the wheat gluten)

5.2. *Scanning Electron Microscopy*

The textured samples can have fibre-based structures (see Figure 1). Figure 7 shows SEM images of fibrous samples. The structures in Figure 7(left) have widths in the range of 150 - 300 μm. Figure 7(left) suggests that the large fibrous structures are made up of smaller ones and that the structures are interconnected with much smaller fibres (1-5 μm diameter). The red box area in Figure 7(left) includes various fibres that form a single bigger fibrous bundle. These fibres are probably gluten. Figure 7(right) shows the surface of the specimen oriented in the H-R plane. Figure 7(right) has been rotated ~35^{o} counter-clockwise with the top left part showing the surface oriented in the H-v plane. In Figure 7(right), the tips of the fibres can be seen; the shape is irregular, which can be attributed to various fibres connected to form a larger one. The red box area in Figure 7(left) highlights the presence of what is thought to be a single gluten fibril.

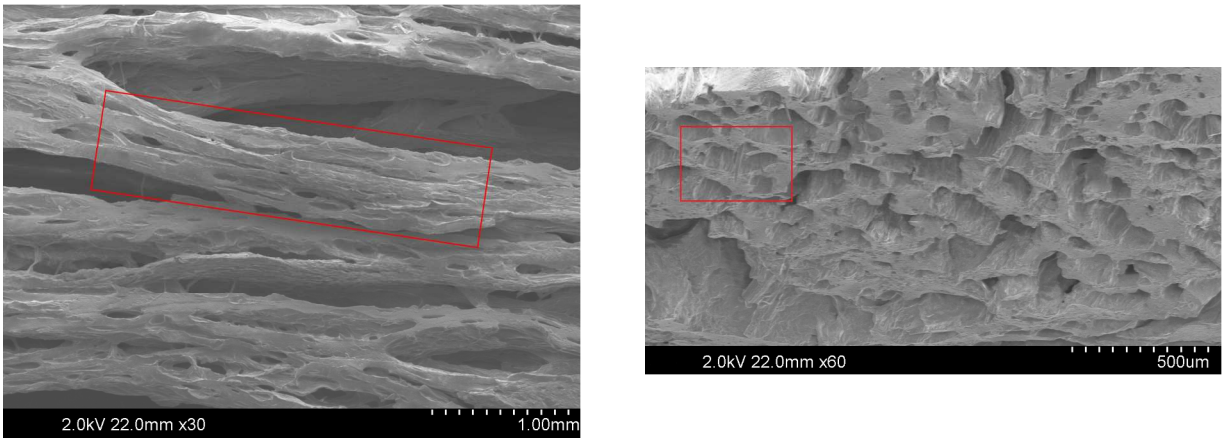

Figure 7: SEM images of a fibrous sample at different view planes; *left*: the displayed surface is oriented in the R-v plane (see Figure 1); *right*: the displayed surface is oriented in the H-R plane (see Figure 1).

5.3. Texture Analysis – Mechanical Testing

The materials selected in this study, (soy protein isolate and vital wheat gluten) have potential to form the basis for a meat replacer. It is therefore interesting to compare the samples obtained with raw meat. To this end, tensile tests were performed on raw beef. All the samples were first frozen for 3 h to make it easier to cut the specimens; then, the specimens were packed in plastic seal bags. The specimens were tested when they reached room temperature.

The results of the tensile tests for raw meat are presented in Figure 8 and compared to a typical fibrous structured sample. The results are presented in terms of the tensile stress and strain parallel and perpendicular to the fibres. In the event of beef, three specimens were tested parallel and perpendicular to the fibres. The anisotropy index is displayed as a blue graph in Figure 8. The anisotropy index is the ratio between the parallel and perpendicular direction (stress or strain); the connecting line between the dots is for visual convenience.

In Figure 8, it is shown that a typical fibrous structured sample obtained, after processing at 95 ^{o}C and 30 RPM for 15 min, has comparable stress and strain anisotropy indices (~2 and ~1.8, respectively) with raw meat (beef). All displayed error bars represent the margin of error at 95% confidence interval. This implies that the meat replacers obtained with the Couette Cell exhibit similar mechanical properties as raw meat. This makes it a promising process to develop the meat replacers.

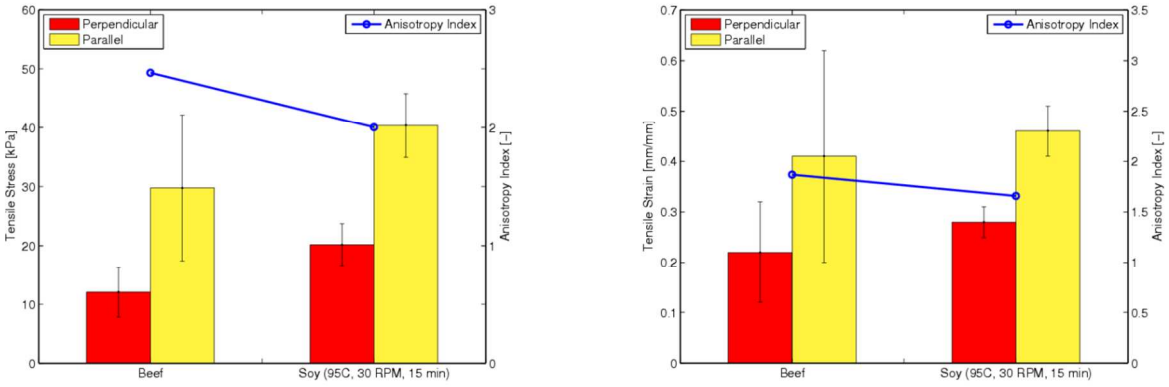

Tensile stress results Tensile strain results

Figure 8: Tensile stress and strain measurements for raw meat (beef) and a typical fibrous structured sample obtained with the Couette Cell.

5.4. Neutron refraction

Figure 9 shows two neutron refraction measurements performed on a sample in which D_2O had replaced H_2O. These measurements were meant to check whether any depolarization would be visible for this type of material. Thicker specimens could contain more layers of fibres and therefore show more depolarization. The experimental data in Figure 9 have been fitted using a fixed realistic value for SLD being $4.3 \cdot 10^{14}$ m^{-2}. This SLD value corresponds to experimental data fitting with the lowest error for n and σ. It also indicates that there is air entrapped in the treated samples as can been seen in Figure 7. The obtained number of layers of fibres (n) is 36 ± 4 for the total specimen thickness of 5 mm and the standard deviation (σ) of the orientation distribution is 0.66 ± 0.04 radians. The thickness of one layer of fibres is 138 µm and this value is in good agreement with the SEM inspection reported in [7] and Figure 7. There is a distinct difference in the depolarization between the vertical and horizontal specimens, providing verification of anisotropic structuring.

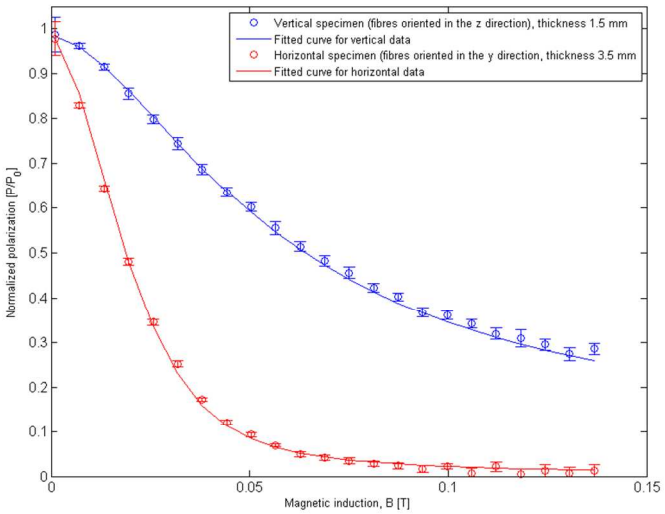

305

306 **Figure 9**: Fitted curve for SESANS measurement data for horizontal and vertical specimens.

307

308 Figure 10 shows how the number of layers of fibres n varies with SLD. This graph is the combined analysis of both
309 vertical and horizontal data of the specimen. Assumptions about the water content of the specimen had to be made to
310 calculate the SLD for meat replacers. As explained earlier, we can define the lower and upper limits of SLD for our
311 system with the lower one being the SPI/air interface of $1.68 \cdot 10^{14}$ m^{-2} and the upper one being the SPI/D_2O interface
312 of $4.7 \cdot 10^{14}$ m^{-2}. Therefore, in Figure 10, SLD is varied within these limits. Figure 10 shows the close relation
313 between n and SLD and that these parameters are completely coupled when both are fitted. This implies that the
314 fibre diameter can be between 30 and 150 µm if our assumptions about the water content were not correct.

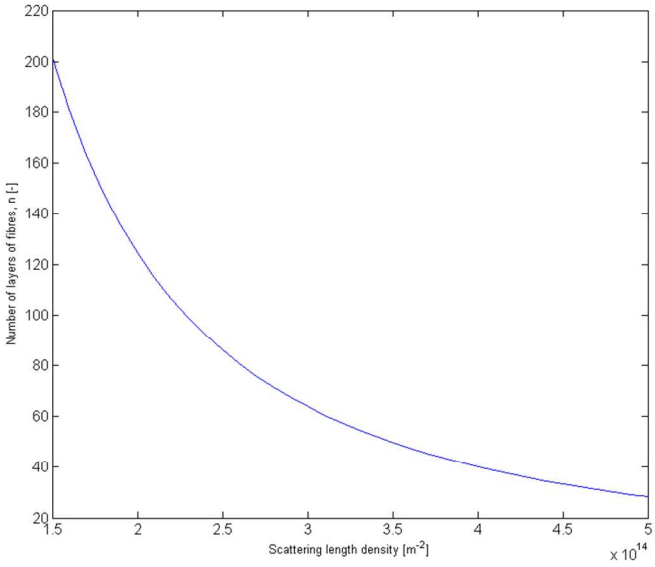

315

316 **Figure 10**: Number of layers of fibres for the sum of both vertical and horizontal measurement data as
317 function of SLD.

318

319 ## *6. Synopsis of complementary characterization techniques*

320 Light microscopy together with SEM provided a detailed view of anisotropic SPI-gluten blend, illustrating the
321 structure formed over the visible or created surfaces. Protein orientation in the direction of the flow was evident and
322 fibrous formation appeared to exist in the macro- and micro-scale. Use of toluidine blue stain moutant enabled visual
323 observation of the SPI and gluten protein distribution using light microscopy. Texture Analysis provided quantitative
324 comparison between raw meat (beef) and the obtained meat replacer. The meat replacer obtained from the Couette
325 Cell after processing at 95 ^{o}C and 30 RPM for 15 min exhibited high stress and strain anisotropy indices (~2 and
326 ~1.8, respectively), comparable to those of raw meat (beef).

327 By employing neutron refraction with the novel SESANS technique, a complementary investigation of the structure
328 formation was enabled. We were able to quantify the number of fibre layers (36 ± 4) and the orientation distribution
329 of fibres (0.66 ± 0.04 radians). The neutron refraction results were in line with SEM observations; specifically, same
330 values were obtained for the sample fibre thickness (138 μm) both with SEM and neutron refraction. The structure
331 formation of the treated sample shown in the light microscopy images follows approximately the same orientation

distribution (± 40°) in the direction of the flow. Perfectly oriented fibres would result in higher anisotropy index values.

7. Conclusions

We have used a range of complementary techniques to characterize plant-based meat replacers, produced in a Couette Cell. The techniques used provided insight into the structures formed at the surface and bulk of the material. Light Microscopy (LM) was used to differentiate between proteins (SPI, gluten) and revealed anisotropic formations in the direction of the flow. Scanning Electron Microscopy (SEM) was used to observe the morphology of the treated biopolymer mixture of SPI-gluten (plant-based meat replacer) at micro-scale. Based on the SEM observations, the fibre thickness was found to be ± 150 μm. Texture Analysis (TA) was done to enable quantitative comparison between the mechanical properties (tensile stress and strain) of raw meat (beef) and the novel meat replacers produced in the Couette Cell. For the treated sample high tensile stress and strain anisotropy indices (~2 and ~1.8, respectively) were found, which are comparable to those of raw meat (beef). Most importantly, a novel technique called spin-echo small angle neutron scattering (SESANS) was used to quantify the number of fibre layers (± 36) in the bulk of the meat replacers (a *look inside* the material). From the number of fibre layers within the tested specimens, the thickness of fibre layers (± 138 μm) was calculated and was found to be in agreement with SEM observations.

As a final note, combinatorial use of several characterization techniques is necessary for better understanding of the nature of plant-based meat replacers as well as their functionality and structuring mechanisms. In this context, common techniques, such as LM, SEM and TA complemented by SESANS can give the full qualitative and quantitative three-dimensional picture of structures formed inside the material.

Acknowledgements

We thank Wim van Oordt and Mojgan Talebi (Department of Product and Process Engineering, TU Delft) for their help obtaining the LM images, Michel van den Brink (Department of Process and Energy, TU Delft) for his help

obtaining the SEM images, Patrick van Holst and Harry Jansen (Department of Precision and Microsystems Engineering, TU Delft) for their help and technical assistance with the texture analysis measurements and Chris Duif (Department of Radiation, Science & Technology, TU Delft) for his technical assistance and collaboration with the SESANS measurements. This research is carried out within the "Intensified Protein Structuring (IPS) for More Sustainable Food" research programme, which is part of the "Institute for Sustainable Process Technology (ISPT)" and supported by "The Peas Foundation (TPF)". The SPI and vital wheat gluten have been kindly provided by Barentz B.V. The meat samples were kindly donated by Slagerij Deken (Wormerveer, The Netherlands).

References

1. H. Steinfield, P. Gerber, T. Wassenaar, V. Castel, Food, A. O. of the United Nations, E. Livestock, D. (Firm) and C. De Haan, *Livestock's long shadow: environmental issues and options*, Food and agriculture organization of the United Nations, 2006.

2. R. K. Pachauri, 2008.

3. A. C. Hoek, P. A. Luning, P. Weijzen, W. Engels, F. J. Kok and C. de Graaf, *Appetite*, 2011, **56**, 662 - 673.

4. J. C. Cheftel, M. Kitagawa and C. Quéguiner, *Food Reviews International*, 1992, **8**, 235-275.

5. D. J. Gallant, B. Bouchet and J. Culioli, *Food Microstruct*, 1984, **3**, 175-183.

6. K. J. Grabowska, S. Tekidou, R. M. Boom and A. J. v. d. Goot, *Food Res Int*, 2014.

7. G. A. Krintiras, J. Göbel, A. J. van der Goot and G. D. Stefanidis, *Food and Bioprocess Technology*, 2014, **under review**.

8. J. M. Aguilera and D. W. Stanley, *Microstructural principles of food processing and engineering*, Aspen Publishers, Gaithersburg, MD, 1999.

9. A. G. Gaonkar, *Characterization of food : emerging methods*, Elsevier, Amsterdam ; New York, 1995.

10. J. Plomp, J. G. Barker, V. O. de Haan, W. G. Bouwman and A. A. van Well, *Nuclear Instruments and Methods in Physics Research Section A: Accelerators, Spectrometers, Detectors and Associated Equipment*, 2007, **574**, 324 - 329.

11. M. T. Rekveldt, J. Plomp, W. G. Bouwman, W. H. Kraan, S. Grigoriev and M. Blaauw, *Rev Sci Instrum*, 2005, **76**.

12. O. Byron and R. J. Gilbert, *Current Opinion in Biotechnology*, 2000, **11**, 72 - 80.

13. S. H. Peighambardoust, S. v. Brenk, A. J. v. d. Goot, R. J. Hamer and R. M. Boom, *J Cereal Sci*, 2007, **45**, 34-48.

14. F. O. Flint and B. M. Firth, *Analyst*, 1988, **113**, 365-366.

15. NIST, NIST Scattering Length Density Calculator.

16. R. P. Singh, R. P. Singh and D. R. Heldman, *Introduction to Food Engineering*, Elsevier Science, 2008.